

# Neutrally Buoyant Particles and Bailout Embeddings in Three-Dimensional Flows

Julyan H. E. Cartwright,<sup>1,†</sup> Marcelo O. Magnasco,<sup>2,‡</sup> Oreste Piro,<sup>3,‡</sup> and Idan Tuval.<sup>3,‡</sup>

<sup>1</sup>*Laboratorio de Estudios Cristalográficos, CSIC, E-18071 Granada, Spain*

<sup>2</sup>*Mathematical Physics Lab, Rockefeller University, Box 212, 1230 York Avenue, NY 10021*

<sup>3</sup>*Institut Mediterrani d'Estudis Avançats, CSIC-UIB, E-07071 Palma de Mallorca, Spain*

(Dated: version of May 21, 2019)

We use the bailout embeddings of three-dimensional volume-preserving maps to study qualitatively the dynamics of small spherical neutrally buoyant impurities suspended in a time-periodic incompressible fluid flow. The accumulation of impurities in tubular vortical structures, the detachment of particles from fluid trajectories near hyperbolic invariant lines, and the formation of nontrivial three-dimensional structures in the distribution of particles are predicted.

PACS numbers: 05.45.Gg, 47.52.+j, 45.20.Jj

The dynamics of small spherical particles immersed in a fluid flow have received considerable attention in the past few years from both the theoretical and experimental points of view. On one hand, these particles are the simplest models for impurities whose transport in flows is of practical interest to understand, and, on the other, their motion is governed by dynamical systems that display a rich and complex variety of behavior even in the case of the most minimal approximations.

When the density of the particles does not match that of the fluid, it is intuitively clear that the trajectories of a particle and a fluid parcel will in general differ. This has been demonstrated in two-dimensional flows in which particles with density higher than the basic flow tend to migrate away from the parts of the flow dominated by rotation — in the case of chaotic flows, the KAM (Kolmogorov–Arnold–Moser) islands — while particles lighter than the fluid display the opposite tendency [1, 2, 3]. A more surprising result, however, is that neutrally buoyant particles may also detach from the fluid parcel trajectories in the regions in which the flow is dominated by strain, with the result that they end up settling in the KAM islands [4]. The subtle dynamical mechanism responsible for the latter phenomenon has suggested a method to target KAM islands in Hamiltonian flows, and a recent generalization named a bailout embedding permits its extension to Hamiltonian maps as well [5].

Despite its obvious importance from the point of view of applications, the case in which the base flow is three-dimensional has been much less investigated. A probable reason for this is the fact that very few simple three-dimensional incompressible flow models exist. The few that are simple are not realistic — e.g., the ABC (Arnold–Beltrami–Childress) flow [6] — and the few that are realistic are far more complex. In the study of the Lagrangian structure of three-dimensional incompressible time-periodic flows, where this difficulty was already present, the alternative approach of qualitatively modeling the flows by iterated three-dimensional volume-preserving maps was successful in predicting fundamental structures that were later found in more realistic theoretical flows and in experiments [7, 8, 9, 10]. However, no similar approach has been followed to describe the motion of impurities in this kind of flows.

This Letter has the dual purpose of extending the idea of bailout embedding to a class of dynamical systems outside the Hamiltonian domain, namely three-dimensional volume-preserving maps, and by means of this embedding investigating the generic structures that one might expect in the dynamics of neutrally buoyant particles suspended in incompressible three-dimensional time-periodic flows.

Let us first recall the equation of motion for a small, neutrally buoyant, spherical tracer in an incompressible fluid (the Maxey–Riley equation) [11, 12]. Under assumptions allowing us to retain only the Bernoulli, Stokes drag, and Taylor added mass contributions to the force exerted by the fluid on the sphere, the equation of motion for the particle at position  $\mathbf{x}$  is

$$\frac{d}{dt}(\mathbf{x} - \mathbf{u}(\mathbf{x})) = (-\mathbf{r} + \mathbf{u}) \cdot (\mathbf{x} - \mathbf{u}(\mathbf{x})); \quad (1)$$

where  $\mathbf{x}$  represents the velocity of the particle,  $\mathbf{u}$  that of the fluid,  $\mathbf{r}$  a number inversely proportional to the Stokes number of the particle, and  $\mathbf{r} \cdot \mathbf{u}$  the Jacobian derivative matrix of the flow.

The difference between the particle velocity and the velocity of the surrounding fluid is exponentially damped with negative damping term  $(-\mathbf{r} + \mathbf{u})$ . In the case in which the flow gradients reach the magnitude of the viscous drag coefficient, there is the possibility that the Jacobian matrix  $\mathbf{r} \cdot \mathbf{u}$  may acquire an eigenvalue of positive real part in excess of the drag coefficient. In these instances, the trajectories of the impurities, instead of converging exponentially onto those defined by  $\mathbf{x} = \mathbf{u}$ , may detach from them.

For incompressible two-dimensional flows, since the Jacobian matrix is traceless, the two eigenvalues must add up to zero, which implies that they are either both purely imaginary or both purely real, mutually equal in absolute value and opposite in sign. The result is that the particles can abandon the fluid trajectories in the neighborhood of the saddle points and other unstable orbits, where the Jacobian eigenvalues are real, and eventually overcome the Stokes drag, to finally end up in a regular region of the flow on a KAM torus dominated by the imaginary eigenvalues. From a more physical point of view, this effect implies that the particles tend to stay away of the

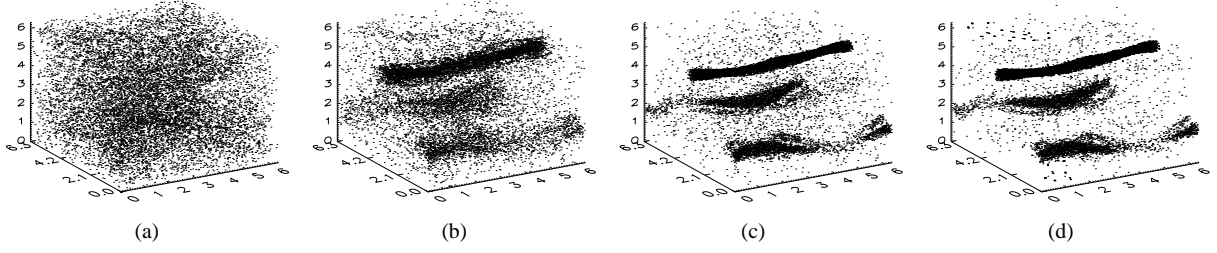


FIG. 1: For a homogeneous distribution of initial conditions we plot only the last 1000 steps of the map evolution for different values of  $\epsilon$ : (a)  $\epsilon = 2$ ; (b)  $\epsilon = 1$ ; (c)  $\epsilon = 0.6$ ; (d)  $\epsilon = 0.5$ . The images represent the  $[0, 2]$  cube in the phase space.

regions of strongest strain.

In contrast to the two-dimensional case, in time-dependent three-dimensional flows the incompressibility condition only implies that the sum of the three independent eigenvalues must be zero. This less restrictive condition allows for many more combinations. Triplets of real eigenvalues, two positive and one negative or vice versa, as well as one real eigenvalue of any sign together with a complex-conjugate pair whose real part is of the opposite sign, are possible. Accordingly, chaotic trajectories may have one or two positive Lyapunov numbers, and a richer range of dynamical situations may be expected.

Instead of investigating all these in terms of a given fully fledged three-dimensional time-periodic model flow, we follow a qualitative approach based on iterated maps that roughly reproduces the properties of the impurity dynamics in a generic flow of this kind. In order to construct the map we first note that the dynamical system governing the behavior of neutrally buoyant particles is composed of some dynamics within another larger set of dynamics. Equation (1) can be seen as an equation for a variable  $\mathbf{x} = (\mathbf{x}_u)$  which in turn will define the equation of motion  $(\mathbf{x} = \mathbf{u})$  of a fluid element whenever the solution of the former be zero. In this sense we may say that the fluid parcel dynamics is embedded in the particle dynamics. In reference to the fact that some of the embedding trajectories abandon some of those of the embedded dynamics, the generalization of this process is dubbed a bailout embedding [5].

It is rather easy to construct this type of embedding for map dynamics. Given a map

$$\mathbf{X}_{n+1} = \mathbf{T}(\mathbf{X}_n); \quad (2)$$

a general bailout embedding is given by

$$\mathbf{X}_{n+2} = \mathbf{T}(\mathbf{X}_{n+1}) = \mathbf{K}(\mathbf{X}_n)(\mathbf{X}_{n+1} - \mathbf{T}(\mathbf{X}_n)); \quad (3)$$

where  $\mathbf{K}(\mathbf{x})$  is the so-called bailout function whose properties determine which trajectories of the embedded map will be eventually abandoned by the embedding. The particular choice — naturally imposed by the particle dynamics — of the gradient as the bailout function in a flow translates in the map setting to

$$\mathbf{K}(\mathbf{x}) = e^{-\mathbf{r} \cdot \mathbf{T}}; \quad (4)$$

Bailout embeddings have been used to investigate targeting of KAM tori in Hamiltonian systems as well as to explore generic properties of the distribution of small particles immersed in incompressible two-dimensional fluid flows [5], which are also of a Hamiltonian nature. Following a similar approach here leads us to consider the bailout embedding of a class of non-Hamiltonian systems: three-dimensional volume-preserving maps. In particular, we chose to represent qualitatively chaotic three-dimensional incompressible base flows periodic in time by ABC maps, a family

$$\mathbf{T} = \mathbf{T}_{ABC} : (\mathbf{x}_n; \mathbf{y}_n; \mathbf{z}_n) \mapsto (\mathbf{x}_{n+1}; \mathbf{y}_{n+1}; \mathbf{z}_{n+1}); \quad (5)$$

where

$$\begin{aligned} \mathbf{x}_{n+1} &= \mathbf{x}_n + A \sin \mathbf{z}_n + C \cos \mathbf{y}_n \pmod{2\pi}; \\ \mathbf{y}_{n+1} &= \mathbf{y}_n + B \sin \mathbf{x}_{n+1} + A \cos \mathbf{z}_n \pmod{2\pi}; \\ \mathbf{z}_{n+1} &= \mathbf{z}_n + C \sin \mathbf{y}_{n+1} + B \cos \mathbf{x}_{n+1} \pmod{2\pi}; \end{aligned} \quad (6)$$

that displays all the basic features of interest of the evolution of fluid flows. Depending on the parameter values, this map possesses two quasi-integrable behaviors: the one-action type, in which a KAM-type theorem exists, and with it invariant surfaces shaped as tubes or sheets; and the two-action type displaying the phenomenon of resonance-induced diffusion leading to global transport throughout phase space [7].

Let us now study the dynamics defined by Eqs (3), (4) and (5). We first concentrate on the cases in which the flow is dominated by one-action behavior. In these we find an interesting generalization of the behavior already found in two dimensions. Particle trajectories are expelled from the chaotic regions to finally settle in the regular KAM tubes. As an example, we take values of  $A$ ,  $B$ , and  $C$  that lead to almost ergodic behavior of the fluid map: a single fluid trajectory almost completely covers the phase space. However, from randomly distributed initial conditions, the particle trajectories inevitably visit some hyperbolic regions where they detach from the corresponding fluid trajectory. In this fashion they find their way inside the invariant elliptic structures where they can finally relax back onto a safe fluid trajectory. In Fig. 1 we show how a homogeneous distribution of one hundred particles in the fluid flow, after a large number of stabilization iterations, finally settles inside the tubular KAM structures for different

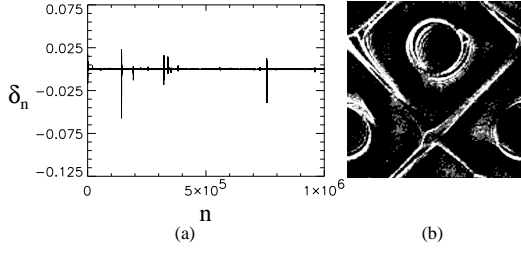


FIG. 2: (a) The evolution of one component of the difference  $\delta_n$  between the particles and the fluid flow velocities as a function of the number of iterations. (b) An  $xy$  slice of the phase space with those points where  $\delta_n$  is greater than  $\delta_0$ . The square is the region  $[0, 2] \times [0, 2]$ .

values of the parameter  $\delta$ . When the value of  $\delta$  decreases, more random trajectories follow this evolution; more particles fall into the invariant tubes.

In the two-action case, the eigenvalues of the Jacobian are very small on large portions of the motion, so that separation may only occur sporadically during the short time intervals in which the fluid parcel crosses the fast motion resonances [7]. Most of the time, particles and fluid parcels follow exponentially convergent trajectories causing the separations to be then practically unobservable except for very small values of  $\delta$ . Most probably, once the particles converge to the fluid dynamics they remain attached. However, by adding a small amount of white noise, we can continually force the impurity to fluctuate around the flow trajectory [13]. From the application point of view, this noise may be considered to represent the effect of small scale turbulence, thermal fluctuations, etc, but here we will use it only as a dynamical device. With this, the particles arrive in the neighborhood of the resonances with a non-negligible velocity mismatch with the fluid that is considerably amplified during the transit across the resonance. The measure of this mismatch is then a good detector of the proximity of the resonance. Let us specifically study the following stochastic iterative system:

$$\mathbf{x}_{n+2} = \mathbf{T}(\mathbf{x}_{n+1}) = \mathbf{e}^{-\mathbf{r} \cdot \mathbf{T}(\mathbf{x}_{n+1} - \mathbf{x}_n)} + \mathbf{n}_n : (7)$$

The noise term  $\mathbf{n}_n$  satisfies

$$\begin{aligned} \langle \mathbf{n}_n \rangle &= \mathbf{0}; \\ \langle \mathbf{n}_n \mathbf{n}_m^T \rangle &= \delta_{nm} \mathbf{I} : \end{aligned} \quad (8)$$

We can recast Eq. (7) into

$$\begin{aligned} \mathbf{x}_{n+1} &= \mathbf{T}(\mathbf{x}_n) + \mathbf{n}_n \\ \mathbf{n}_{n+1} &= \mathbf{e}^{-\mathbf{r} \cdot \mathbf{T}(\mathbf{x}_{n+1} - \mathbf{x}_n)} + \mathbf{n}_n \end{aligned} \quad (9)$$

if we define the velocity separation between the fluid and the particle as  $\delta_n = \|\mathbf{x}_{n+1} - \mathbf{T}(\mathbf{x}_n)\|$ .

Let us illustrate the behavior referred above by studying the most ergodic two-action case in which all the fluid trajectories intersect the resonant lines. In Fig. 2a we show how  $\delta_n$  grows

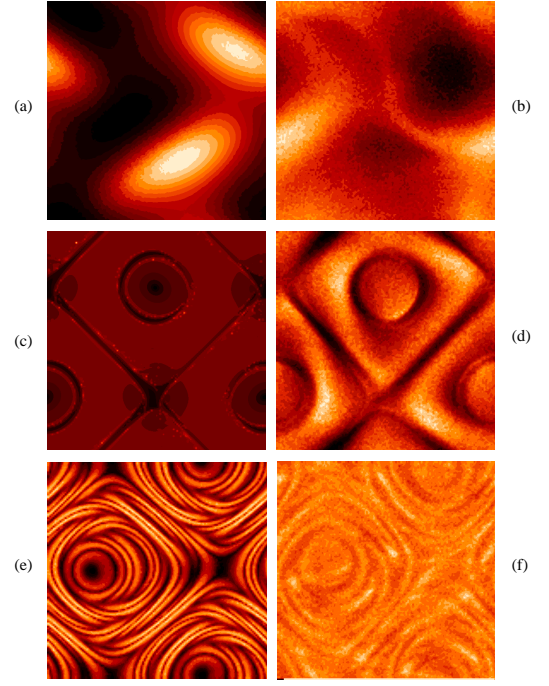


FIG. 3: The temperature amplitude for the one-action, two-action and most chaotic cases ((a), (c), and (e) respectively), together with the corresponding slices of the impurity dynamics (histogram) in the phase space ((b), (d), and (f)). All images are the  $[0, 2] \times [0, 2]$  region in the  $xy$  axis, for a slice in the  $z$  direction corresponding to the values  $z \in [0, 0.49]$ .

strongly at some points. These points correspond to the crossings of the resonant lines. In Fig. 2b we plot these points in an  $xy$  slice of the three-dimensional cube, choosing those points where the value of  $\delta_n$  is greater than a certain minimum value  $\delta_0$ . As shown, we recover the resonant structure previously noted [7, 8].

This is the most primitive way to obtain useful information from the noisy particle dynamics. A shrewder analysis [13] shows how the variance of the separation  $\delta_n$  between particles and fluid trajectories and the variance of the noise  $\mathbf{n}_n$  are related by a function that only depends on the particular point of the phase space that we look at, in a sort of temperature amplitude for the fluctuations of  $\delta$ ,

$$T(\mathbf{x}) = \frac{\langle \delta^2 \rangle}{h^2} = \frac{\mathbf{x}^T \mathbf{e}^{-\mathbf{r} \cdot \mathbf{T}(\mathbf{x})} \mathbf{r} \cdot \mathbf{T}(\mathbf{x})}{h^2} : \quad (10)$$

This amplitude takes different values at different points of the flow. At those points that the particle dynamics tries to avoid, its value increases, so the particle prefers to escape the hot regions and to fall into the cold ones.

In Fig. 3 we show this phenomenon. First we analyze a one-action situation showing the temperature amplitude, as well as the impurity dynamics (Figs 3a and 3b respectively). Again we use slices of the three-dimensional cube to show the situation more clearly. Fig. 3a shows the temperature in

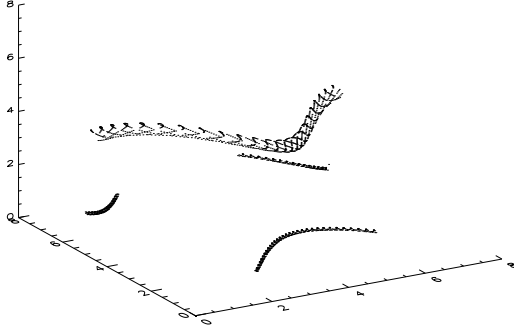


FIG. 4: Stroboscopic sampling ( $\tau=1$ ) of the position of 10 particles initially distributed at random in a flow described by Eq. (11) with  $A = 2$ ,  $B = 0.4$ , and  $C = 1.2$ . The dots represent the positions of these particles at the strobing periods 1000 to 2000.

a scaled color code (lighter is hotter). Fig. 3b shows a histogram of visits that a single particle pays to each bin of the space. The agreement between the higher temperature regions and the less visited ones is evident. Next we plot the same pictures but in the two-action case studied before (Figs 3c and 3d). Finally, we apply this analysis to a generic chaotic case where we do not have any information about the phase space structure. We show in Fig. 3e how the invariant manifolds are very twisted, and in Fig. 3f how the particles, even so, try to find the coldest regions of the flow.

In order to show that the above described behavior is not an artefact of our mapping-based approach, we have performed analogous simulations using a continuous-time model as a base flow. Specifically we have considered neutrally buoyant particles immersed in a modified version of the ABC flow, in which each component of the velocity vector field is sinusoidally modulated with a relative phase shift of  $2\pi/3$  and where  $x$ ,  $y$ , and  $z$  are to be considered ( $\text{mod } 2\pi$ )

$$\begin{aligned}\frac{dx}{dt} &= (1 + \sin 2\pi t) (A \sin z + C \cos y); \\ \frac{dy}{dt} &= (1 + \sin 2\pi (t + \frac{1}{3})) (B \sin x + A \cos z); \\ \frac{dz}{dt} &= (1 + \sin 2\pi (t + \frac{2}{3})) (C \sin y + B \cos x); \end{aligned} \quad (11)$$

While a detailed analysis of the dynamical aspects of this flow is beyond the scope of this Letter, we anticipate that it shows structures similar to those of the ABC maps, i.e., a complex array of KAM sheets and tubes surrounded by chaotic volumes. Neutrally buoyant particles evolved according to the true (simplified) Maxey–Riley equations, Eq. (1), based on this flow, show exactly the same tendency to accumulate inside KAM tubes as in the map case. This is depicted in Fig. 4, where ten particles, initially distributed at random in the cubic cell, are shown to end up in the interior of two of the tubes mentioned above.

This confirmation demonstrates the validity of the qualitative approach based on the bailout embedding of three-dimensional volume-preserving maps to describe the dynamics of neutrally buoyant particles immersed in three-dimensional time-periodic incompressible flows. This application of the bailout concept is the first to be reported for a non-Hamiltonian dynamical system. Our approach can be pursued with two different goals in mind: on one hand, it contributes to the understanding of the physical behavior of impurities, and on the other hand, it provides a mathematical device to learn about the dynamical structures of the base flow in situations where these are very difficult to elucidate directly. Notice that both bodies of information are very important to improve our presently scarce knowledge of the transport properties of three-dimensional fluid flows.

This research was performed by IT as part of his doctoral thesis under the supervision of OP, together with additional input from JHEC and MOM. JHEC acknowledges the financial support of the Spanish CSIC, Plan Nacional del Espacio contract PNE-007/2000-C, MOM acknowledges the support of the Meyer Foundation, and OP and IT acknowledge the Spanish Ministerio de Ciencia y Tecnología, Proyecto CONOCE, contract BFM2000-1108 and Proyecto IMAGEN, contract REN2001-0802-C02-01.

URL: <http://lec.ugr.es/~julyan>; Electronic address: [julyan@lec.ugr.es](mailto:julyan@lec.ugr.es)

<sup>y</sup> URL: <http://asterion.rockefeller.edu/marcelo/>; Electronic address: [marcelo@sur.rockefeller.edu](mailto:marcelo@sur.rockefeller.edu)

<sup>z</sup> URL: <http://www.imedeauib.es/~piro>; Electronic address: [piro@imedeauib.es](mailto:piro@imedeauib.es)

<sup>x</sup> URL: <http://www.imedeauib.es/~idan>; Electronic address: [idan@imedeauib.es](mailto:idan@imedeauib.es)

- [1] A. Crisanti, M. Falcioni, A. Provenzale, and A. Vulpiani, *Phys. Lett. A* **150**, 79 (1990).
- [2] P. Tanga and A. Provenzale, *Physica D* **76**, 202 (1994).
- [3] A. Babiano, J. H. E. Cartwright, O. Piro, and A. Provenzale, in *Coherent Structures in Complex Systems*, edited by D. Reguera, L. Bonilla, and M. Rubi (Springer, 2001), vol. 567 of *Lecture Notes in Physics*, pp. 114–126.
- [4] A. Babiano, J. H. E. Cartwright, O. Piro, and A. Provenzale, *Phys. Rev. Lett.* **84**, 5764 (2000).
- [5] J. H. E. Cartwright, M. O. Magnasco, and O. Piro, *Phys. Rev. E* **to appear** (2002).
- [6] V. I. Arnold, *C. R. Acad. Sci. Paris A* **261**, 17 (1965).
- [7] M. Feingold, L. P. Kadanoff, and O. Piro, *J. Stat. Phys.* **50**, 529 (1988).
- [8] O. Piro and M. Feingold, *Phys. Rev. Lett.* **61**, 1799 (1988).
- [9] J. H. E. Cartwright, M. Feingold, and O. Piro, *Physica D* **76**, 22 (1994).
- [10] J. H. E. Cartwright, M. Feingold, and O. Piro, *J. Fluid Mech.* **316**, 259 (1996).
- [11] M. R. Maxey and J. J. Riley, *Phys. Fluids* **26**, 883 (1983).
- [12] E. E. Michaelides, *J. Fluids Eng.* **119**, 233 (1997).
- [13] J. H. E. Cartwright, M. O. Magnasco, and O. Piro, *Chaos* **submitted** (2002).